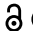



ORIGINAL RESEARCH

 OPEN ACCESS 

## Lymphatic endothelial cell-mediated accumulation of CD177<sup>+</sup>Treg cells suppresses antitumor immunity in human esophageal squamous cell carcinoma

Min Ma<sup>a,b,\*</sup>, Liang Li<sup>c\*</sup>, Shu-Han Yang<sup>b</sup>, Chuan Huang<sup>a,b</sup>, Weitao Zhuang<sup>d</sup>, Shujie Huang<sup>d</sup>, Xin Xia<sup>d</sup>, Yong Tang<sup>d</sup>, Zijun Li<sup>e</sup>, Zhi-Bin Zhao<sup>c</sup>, Qingyun Chen<sup>c</sup>, Guibin Qiao<sup>d</sup>, and Zhe-Xiong Lian<sup>a,b</sup>

<sup>a</sup>Chronic Disease Laboratory, School of Medicine South China University of Technology, Guangzhou, China; <sup>b</sup>Guangdong Provincial People's Hospital (Guangdong Academy of Medical Sciences), Southern Medical University, Guangzhou, China; <sup>c</sup>Medical Research Institute, Guangdong Provincial People's Hospital (Guangdong Academy of Medical Sciences), Southern Medical University, Guangzhou, China; <sup>d</sup>Department of Thoracic Surgery, Guangdong Provincial People's Hospital (Guangdong Academy of Medical Sciences), Southern Medical University, Guangzhou, China; <sup>e</sup>Guangdong Provincial Institute of Geriatrics, Concord Medical Center, Guangdong Provincial People's Hospital (Guangdong Academy of Medical Sciences), Southern Medical University, Guangzhou, China

### ABSTRACT

Regulatory T (Treg) cells are critical in shaping an immunosuppressive microenvironment to favor tumor progression and resistance to therapies. However, the heterogeneity and function of Treg cells in esophageal squamous cell carcinoma (ESCC) remain underexplored. We identified CD177 as a tumor-infiltrating Treg cell marker in ESCC. Interestingly, expression levels of CD177 and PD-1 were mutually exclusive in tumor Treg cells. CD177<sup>+</sup> Treg cells expressed high levels of IL35, in association with CD8<sup>+</sup> T cell exhaustion, whereas PD-1<sup>+</sup> Treg cells expressed high levels of IL10. Pan-cancer analysis revealed that CD177<sup>+</sup> Treg cells display increased clonal expansion compared to PD-1<sup>+</sup> and double-negative (DN) Treg cells, and CD177<sup>+</sup> and PD-1<sup>+</sup> Treg cells develop from the same DN Treg cell origin. Importantly, we found CD177<sup>+</sup> Treg cell infiltration to be associated with poor overall survival and poor response to anti-PD-1 immunotherapy plus chemotherapy in ESCC patients. Finally, we found that lymphatic endothelial cells are associated with CD177<sup>+</sup> Treg cell accumulation in ESCC tumors, which are also decreased after anti-PD-1 immunotherapy plus chemotherapy. Our work identifies CD177<sup>+</sup> Treg cell as a tumor-specific Treg cell subset and highlights their potential value as a prognostic marker of survival and response to immunotherapy and a therapeutic target in ESCC.

### ARTICLE HISTORY

Received 6 October 2023  
Revised 30 January 2024  
Accepted 4 March 2024

### KEYWORDS

Anti-PD-1 immunotherapy; esophageal squamous cell carcinoma; regulatory T cell; tumor microenvironment; CD177; Lymphatic endothelial cell

## Introduction

ESCC is a common form of esophageal cancer, accounting for more than 90% of cases worldwide.<sup>1</sup> ESCC is a highly aggressive cancer that is often diagnosed at advanced stages. Despite advances in treatment, the overall survival rate of ESCC patients remains low, highlighting the need for a better understanding of the disease. The immunosuppressive microenvironment is important in promoting tumor growth and metastasis in ESCC.<sup>2</sup> Regulatory T (Treg) cells play a critical role in immune suppression in the tumor microenvironment; however, their function in ESCC is poorly understood.


Treg cells assist in tumor immune evasion mainly by secreting suppressive cytokines and expressing inhibitory receptors,<sup>3</sup> which inhibit antitumor T-cell and NK cell activation. Similar to tumor antigen-specific cytotoxic T cells, which are crucial in antitumor immunity, only a subset of Treg cells is critical in suppressing antitumor immunity during tumor progression.<sup>4</sup> An increasing number of studies have reported unique subsets of Treg cells that contribute to tumor growth. CCR8<sup>+</sup> Treg cells

suppress the antitumor immune response in colon cancer, and targeting CCR8 enhances the vaccine-induced tumor-specific response.<sup>5</sup> PD-1<sup>+</sup> Treg cells are key elements that account for poor clinical outcomes in gastric cancer.<sup>6</sup> TIGIT, another immune-suppressive receptor, marks a highly suppressive population of Treg cells, maintaining their suppressive function in melanoma.<sup>7</sup> Similarly, LAG3<sup>+</sup> Treg cells are highly enriched in head and neck squamous cell carcinoma and exhibit enhanced suppressive function compared with their counterpart in peripheral blood.<sup>8</sup> However, the heterogeneity of Treg cells in ESCC is still unclear and needs further investigation.

Although an immunosuppressive microenvironment exists in tumors, promising outcomes of immunotherapies directed at boosting in situ tumor antigen-reactive T-cell expansion and promoting formation of an antitumor immune ecosystem in various tumor types have been reported.<sup>9–12</sup> On the other hand, neoadjuvant immunotherapies utilizing PD-1- or CTLA-4-blocking antibodies have

**CONTACT** Liang Li  [liliang@gdph.org.cn](mailto:liliang@gdph.org.cn)  Medical Research Institute, Guangdong Provincial People's Hospital (Guangdong Academy of Medical Sciences), Southern Medical University, Guangzhou 510080, China; Guibin Qiao  [guibinqiao@126.com](mailto:guibinqiao@126.com)  Department of Thoracic Surgery, Guangdong Provincial People's Hospital (Guangdong Academy of Medical Sciences), Southern Medical University, Guangzhou 510080, China; Zhe-Xiong Lian  [zxlian@gdph.org.cn](mailto:zxlian@gdph.org.cn)  Guangdong Provincial People's Hospital (Guangdong Academy of Medical Sciences), Southern Medical University, Guangzhou 510080, China

\*These authors contributed equally to this work.

 Supplemental data for this article can be accessed online at <https://doi.org/10.1080/2162402X.2024.2327692>

© 2024 The Author(s). Published with license by Taylor & Francis Group, LLC.

This is an Open Access article distributed under the terms of the Creative Commons Attribution-NonCommercial License (<http://creativecommons.org/licenses/by-nc/4.0/>), which permits unrestricted non-commercial use, distribution, and reproduction in any medium, provided the original work is properly cited. The terms on which this article has been published allow the posting of the Accepted Manuscript in a repository by the author(s) or with their consent.

enabled surgery for many locally advanced unresectable tumors,<sup>13,14</sup> including ESCC.<sup>15,16</sup> Neoadjuvant immunotherapies have led to promising clinical benefits in ESCC, such as 31.4% pathological complete response and 48.9% major pathological response.<sup>17</sup> However, some patients do not respond to immunotherapies, and in some cases, PD-1 immunotherapy can even cause tumor hyperprogression.<sup>18</sup> Various studies have reported that tumor-infiltrating Treg cells contribute to resistance to PD-1 therapy and tumor hyperprogression,<sup>6,19</sup> but whether and how Treg cells contribute to the response to immunotherapies in ESCC remain unclear.

In this study, we characterized tumor-infiltrating Treg cells within ESCC and identified a unique tumor-associated CD177<sup>+</sup> Treg cell subset with a suppressive function via mechanisms distinct from those of PD-1<sup>+</sup> Treg cells. CD177<sup>+</sup>Treg cells exist in various cancer types and have a distinct developmental trajectory from PD-1<sup>+</sup> Treg cells. Importantly, CD177<sup>+</sup> Treg cells, rather than PD-1<sup>+</sup> Treg cells, were associated with a poor survival rate and, most interestingly, poor response to neoadjuvant anti-PD-1 immunotherapy in ESCC. Finally, we found that CD31 expression on lymphatic endothelial cells was associated with CD177<sup>+</sup> Treg cell accumulation in the tumor micro-environment. Our work highlights CD177<sup>+</sup> Treg cells as a prognostic marker for survival and response to immunotherapy in ESCC.

## Methods

### Human tumor specimens and single-cell suspension preparation

ESCC clinical samples were obtained from Guangdong Provincial People's Hospital and preprocessed under proper medical protection. Clinical information of ESCC patients were obtained from medical records and listed in supplementary table S1. Clinical stage was classified or reclassified according to the American Joint Committee of Cancer eighth edition ESCC staging system. Survival and response to neoadjuvant immunotherapy plus chemotherapy were defined according to the Response Evaluation Criteria in Solid tumors version 1.1 (RECIST 1.1). This study was approved by the Institutional Review Board of Guangdong Provincial People's Hospital (No. GDREC2019687H). Written informed consent was obtained from each participant.

PBMCs were isolated with Lymphoprep<sup>TM</sup> (STEMCELL Technologies, Vancouver, Canada) density gradient centrifugation. Tumor tissue, tumor-adjacent tissue and remote normal esophageal tissue were cut into 1 mm<sup>3</sup> pieces on ice. The tissue fragments were resuspended in RPMI 1640 (Cytiva HyClone, MA, USA) and filtered through a 75 µm strainer. Collagenase IV (Merck KGaA, Darmstadt, Germany) was added to tissues remaining on the strainer at a 1 mg:200 µl ratio and digested at 37°C for 30 minutes. Digestion was terminated with RPMI 1640 containing 10% FBS (ExCell Bio, Shanghai, China). The digestion mixture was filtered through a 75 µm strainer and mixed with the above cell suspension.

### Flow cytometry

Single-cell suspensions were incubated with mouse serum for 20 minutes at 4°C and then stained with a cocktail of fluorochrome-conjugated antibodies for 20 minutes at 4°C. The monoclonal antibodies used included human α-CD45-APC-Cy7 (2D1; BioLegend, CA, USA), α-CD3-BV510 (OKT3; BioLegend), α-CD56-BV785 (5.1H11; BioLegend), α-CD8a-Alexa Fluor 700 (HIT8a; BioLegend), α-CD4-BUV563 (SK3; BD), α-CD127-BUV737 (HIL-7 R-M21; BD), α-CD25-PE-Cy5 (BC96; BioLegend), α-PD-1-BV421 (EH12.2H7; BioLegend), α-IGG4-PE (HP6025; SouthernBiotech, AL, USA), and α-CD177-FITC (MEM-166; BioLegend). Samples were washed with 0.2% BSA PBS twice and resuspended in 200 µl volume. Cell viability were identified by DAPI staining. Data were acquired with a BD Fortessa SORP flow cytometer (BD Biosciences) and analyzed by FlowJo software (V10, BD Biosciences).

### Elisa

DN, PD-1<sup>+</sup> and CD177<sup>+</sup>Treg cells were sorted from ESCC tumor and tumor-adjacent tissues. These cells were then seeded in a 96-well round bottom plate (3799, Corning), which had been precoated overnight at 4°C with 2 µg/ml of anti-human CD3 (OKT3, BioLegend), at a density of 4,000 cells per well. To stimulate the cells, 1 µg/ml anti-human CD28 (CD28.2, BioLegend) and 50 units/ml hIL-2 (200-02, PEPROTECH) at were added. After a stimulation period of 72 hours, the supernatants were collected for IL-10 (CSB-E04593h, CUSABIO) and IL-35 (CSB-E13126h, CUSABIO) ELISA assay.

### Cell lines and cell culture

Human ESCC cell line KYSE-150 and primary human LECs were purchased from Procell (Wuhan, China). T25 culture flasks (707001, NEST) were coated with 0.1 mg/ml poly-L-lysine (PB180522, Procell) at 37°C for one hour. Human LEC were then seeded at a density of 0.5 million cells per flask. KYSE-150 was cultured with 10% FBS RPMI/F12 medium (32160801, Sigma-Aldrich) and human LECs were cultured with ECM medium (CM-H026, Procell) in a humidified incubator at 5% CO<sub>2</sub> and 37°C.

### LEC adhesion assay

The adhesion capacity of Treg cells were characterized as previously described.<sup>20</sup> Briefly, primary human LECs (CP-H026, Procell) were seeded in a 96-well flat bottom plate (3598, Corning) at a density of 0.1 million cells per cell. Upon reaching 80% confluence, the cells were treated with 0.22 µm-filtered supernatant from the human ESCC cell line (KYSE-150, Procell) for 10 hours. Subsequently, cells isolated from tumor and tumor-adjacent tissue were resuspended in T cell medium containing 50 units/ml of hIL-2 (200-02, PEPROTECH) and 0.5 million cells were added into each well containing the treated LECs. The co-culture was maintained for 5 hours then flipped the plate, followed by trypsinization into a single-cell

suspension. Flow cytometry analysis was performed before and after the co-culture to assess the percentages of three Treg cell subsets.

### **Immunohistochemistry**

Paraffin-embedded tissues were sliced into 4  $\mu\text{m}$  sections and processed with a PDOne 6-color kit (Panovue, Beijing, China) according to the manufacturer's instructions. Slices were subjected to heat-induced antigen retrieval, blocked with 10% goat serum containing TBST, and incubated with primary antibodies. After washing with phosphate-buffered saline containing 0.1% Tween-20, the slices were incubated with HRP-conjugated secondary antibodies, washed and incubated with TSA dyes. After nucleic acid staining with DAPI (Beyotime), the sliced sections were imaged with a Vectra<sup>®</sup> Polaris<sup>™</sup> Automated Quantitative Pathology Imaging System (Akoya Biosciences). The antibodies used included anti-FOXP3 (1:100, 98377S, CST), anti-PD-1 (1:100, 43248, CST), anti-CD177 (1:2000, EPR22813-205, Abcam), and anti-CD31 (1:50, Ab28364, Abcam), anti-LYVE1 (1:20000, Ab14917, Abcam). Images quantification and distance analysis was conducted by HALO image analysis platform 3.6.4134 software (Indica Labs, NM, USA).

### **Single-cell RNA sequence data preprocessing and analysis**

ESCC single-cell RNA sequence data were obtained from Gene Expression Omnibus (GEO) database with accession number GSE160269.<sup>21</sup> The raw count matrix comprised CD45<sup>+</sup> cells and CD45<sup>-</sup> cells from 64 patients. All patients were treated with surgery only. Single-cell RNA sequence data of 4NQO-induced mouse ESCC model were obtained from GSA (Genome Sequence Archive in BIG Data Center, Beijing Institute of Genomics, Chinese Academy of Sciences) with the accession number CRA002118. Pan-cancer data containing the raw count matrix and VDJ sequence profile were obtained from GEO database with accession number GSE156728.<sup>22</sup> Single-cell RNA sequencing data of oral cancer were obtained from GEO database with accession number GSE200996<sup>23</sup> and included Breast Cancer (BC), B cell Lymphoma (BCL), Esophageal Cancer (ESCA), Multiple Myeloma (MM), Pancreatic Cancer (PACA), Renal Carcinoma (RC), Thyroid Carcinoma (THCA), Endometrial Carcinoma (UCEC). The raw count matrix was transformed into a Seurat object and subjected to normalization, and genes that were expressed less than 200 per cell or more than 6000 per cell were removed.

For unsupervised clustering, the top 2000 highly variable features were applied for FindVariableFeatures. For semi-supervision reduction, FindVariableFeatures was conducted using genes specifically expressed by PD-1<sup>+</sup> and CD177<sup>+</sup> Treg cells (Table S3). Then, neighboring genes were located in two-dimensional t-distributed stochastic neighbor embedding (t-SNE) or uniform manifold approximation and projection (UMAP). Cluster-specific gene heatmaps were generated with the DoHeatmap function in the Seurat package (Version 4.3.0).<sup>24-26</sup>

### **Gene ontology (GO) analysis**

Cluster/cell-type-specific genes of unsupervised ESCC Treg Seurat objects were identified by FindAllMarkers. Cluster/cell-type-specific genes were then transformed into Entrez genes using the bitr function. GO analysis was performed using these Entrez genes with the enrichGO function based on GO biological process (GO: BP) datasets. Every single function was obtained using the clusterProfile package (Version 4.6.2).<sup>27,28</sup> The *p* value cutoff was 0.05, and the top five pathways were displayed.

### **Pseudotime trajectory analysis**

To delineate the dynamic differentiation of Treg cells, we performed pseudotime analysis based on Monocle3 (Version 1.2.9)<sup>29</sup> with default setting. Treg cells were embedded in the UMAP trajectory, and pseudotime lineages were assigned to individual cells. Pseudotime-associated functions were obtained from the monocle3 package.

### **T-cell receptor (TCR) clonotype analysis**

We identified the top 10 most abundant TCR clonotype Tregs in pancancer data, divided them into different clone levels according to relative abundance, and compared them with common clonotypes based on chain sequencing. All processes were performed with the scRepertoire package (Version 1.8.0).<sup>30</sup>

### **RNA microarray data and analysis**

ESCC RNA microarray data and proteome mass spectrometry (MS) data were obtained from the GEO database (GSE53625) and ProteomeXchange (PXD021701),<sup>31</sup> respectively. The microarray matrix was assigned gene symbols according to GPL18109 annotation documents. The expression matrix was scaled and normalized by limma package (Version 3.52.2). Difference analysis were performed and differentially expressed gene were used for further analysis.

### **Deconvolution of microarray and MS data**

We extracted count data from single-cell RNA sequencing data included three cluster Treg cells and granulocytes, replaced the cell barcode with the cell type name to form a single-cell reference matrix, uploaded the matrix to Cibersortx (<https://cibersortx.stanford.edu/upload.php>) and calculated the signature matrix by Create Signature Matrix option. This step generated a gene weight matrix, where the rows are gene names, and each cell type is assigned a weight for each gene. Ultimately, this Signature Matrix is used to score the microarray data, providing a relative content assessment of the corresponding cell types in each sample. The Cibersortx algorithms which based on support vector machines (SVMs) will then calculate the relative abundance of each cell type in each sample and assigns scores. Following this, we categorize these scores into high and low groups based on the peaks and valleys observed in the histograms.

### Overall survival-time trajectory analysis

Data for ESCC patients (172 samples for microarray data and 124 samples for MS data) were deconvoluted, and the patients were divided into CD177<sup>+</sup> Treg<sup>hi</sup> and CD177<sup>+</sup> Treg<sup>lo</sup> cohorts according to the median expression level of the CD177<sup>+</sup> Treg cell gene signature. Patients were also divided into PD-1<sup>+</sup> Treg<sup>hi</sup> and PD-1<sup>+</sup> Treg<sup>lo</sup>, DN Treg<sup>hi</sup> and DN Treg<sup>lo</sup> cohorts according to the median expression level of gene signatures of the corresponding cell subset. Overall survival (OS) and disease-free survival (DFS) analyses were carried out using follow-up information and then visualized by the survminer package (Version 0.4.9).

### Statistical analysis

Statistical significance was analyzed using GraphPad Prism 8 (GraphPad Software, San Diego, CA). The results in all figures are expressed as the mean  $\pm$  SD. For comparison of data from multiple groups, statistics were analyzed using one-way ANOVA. Student's t test was used for comparison of data for two groups. For the survival study, Kaplan–Meier survival analysis and the log-rank test were used to determine statistical significance. For the comparison of Treg subset percentage from tumor with different treatments, statistics were analyzed using Mann-Whitney test. Significant differences are indicated as \*  $p < 0.05$ ; \*\*  $p < 0.01$ ; \*\*\*  $p < 0.001$ .

## Results

### Characterization of tumor Treg-specific gene expression in ESCC

To understand tumor Treg cell characteristics in ESCC, we reanalyzed publicly available ESCC single-cell RNA sequencing data (GSE160269)<sup>21</sup> and identified Treg cells according to expression of FOXP3 and CD4 after unsupervised clustering of T/NK cells (Figure 1a,b). We found that Treg cells were enriched in tumor tissue, which is a hallmark of the tumor microenvironment (Figure 1c). Comparing differential gene expression between tumor-infiltrating Treg (T-Treg) and tumor-adjacent Treg (N-Treg) cells (Supplementary table S2), we found upregulation of several genes associated with Treg cell suppressive function in T-Treg cells, such as TNFRSF4 and TNFRSF18 (Figure 1d), which are costimulatory molecules expressed on effector Treg cells. T-Treg cells also show upregulated expression of SOX4, which interacts with TGF- $\beta$  and increases expression of CD39.<sup>32</sup> Moreover, T-Treg cells highly express CD7, which plays an important role in T-cell activation.<sup>33</sup> Interestingly, T-Treg cells highly expressed CD177 and LY6E, two myeloid-derived markers (Figure 1d). Gene ontology (GO) enrichment analysis showed upregulation in T-Treg cells of genes involved in the IL-10 and IL-12 production pathways (Figure 1e). Consistent with other tumor types, our results indicate that T-Treg cells have a high suppressive function in ESCC.

As a Treg cell-specific transcription factor, FOXP3 regulates expression of genes that are critical for maintaining their suppressive function.<sup>34</sup> Therefore, we performed correlation analysis of the gene expression profile of tumor-infiltrating Treg

cells and identified the top 50 genes that correlated positively with FOXP3 expression. Meanwhile, we conducted differential gene expression analysis of Treg cells and non-Treg immune cells and identified top 20 genes that are upregulated in Treg cells. Through intersection of these two groups of genes, we identified 17 genes (Figure 1f). Sorting according to the Pearson correlation coefficient with FOXP3 expression, we found that IL2RA, a well-recognized Treg cell marker, ranked at the top (Figure 1g). Among the upregulated genes, we identified the immune checkpoint molecules CTLA4 and ICOS, which are highly expressed in activated Treg cells. Based on intersection of these 17 genes with upregulated genes in T-Treg cells compared with N-Treg cells in ESCC (Figure 1f), we identified CD177 and CD7 as the top 2 genes, suggesting their important role in tumor Treg function in ESCC (Figure 1g).

### CD177 marks a unique Treg cell subset enriched in ESCC tumor tissue

We then reanalyzed the Treg cell population and found CD177 to be co-expressed with FOXP3 (Figure 2a,b). CD177 was expressed in T-Treg cells, but N-Treg cells expressed low levels of CD177 and FOXP3 (Figure 2c). CD177 is reported to be expressed on activated granulocytes and function as an adhesion molecule by binding its ligand CD31.<sup>35</sup> Recent studies reported that CD177 is also expressed by tumor Treg cells and contributes to Treg suppressive function.<sup>36,37</sup> To reveal the CD177 expression pattern, we reanalyzed immune cell subsets in ESCC. Cell type characterization was performed based on marker genes (Fig. S1). We found that Tregs were the only subset to express CD177 at the transcriptional level (Figure 2d,e). However, we found that granulocytes express CD177 mRNA in another ESCC scRNA-seq data (GSE145370),<sup>38</sup> although the expression level is much lower than in Treg cells (Fig. S2A-C). Flow cytometry analysis of tumor-infiltrating immune cells demonstrated that a high proportion of granulocytes and Treg cells expressed CD177 (Figure 2f, S2D). Moreover, CD177 expression was restricted to tissue Treg cells and increased in T-Treg cells, whereas Treg cells in PBMCs did not express CD177 (Figure 2g,h). On the other hand, the percentage of CD177<sup>+</sup> granulocytes showed no difference between PBMC, normal tissue, tumor-adjacent tissue, and tumor tissue (Figure 2i). Unfortunately, we didn't find CD177 mRNA expression in Treg cells from 4NQO-induced mouse ESCC tumor samples (Fig. S2E-G). In summary, we found a unique CD177<sup>+</sup> Treg cell subset enriched in ESCC tumor tissue with high FOXP3 expression, indicating its critical role in ESCC.

### PD-1<sup>+</sup> Treg and CD177<sup>+</sup> Treg represent two distinct Treg cell subsets in ESCC

Various studies have reported that tumor-infiltrating PD-1<sup>+</sup> Treg cells (CD25<sup>+</sup>CD4<sup>+</sup>FOXP3<sup>hi</sup>) are a highly suppressive Treg subset that contributes to tumor progression<sup>39</sup> as well as to tumor hyper-progression during anti-PD-1 immunotherapy.<sup>6</sup> We examined whether PD-1 is expressed in CD177<sup>+</sup> Treg cells. Interestingly, we found that CD177<sup>+</sup> Treg cells did not express

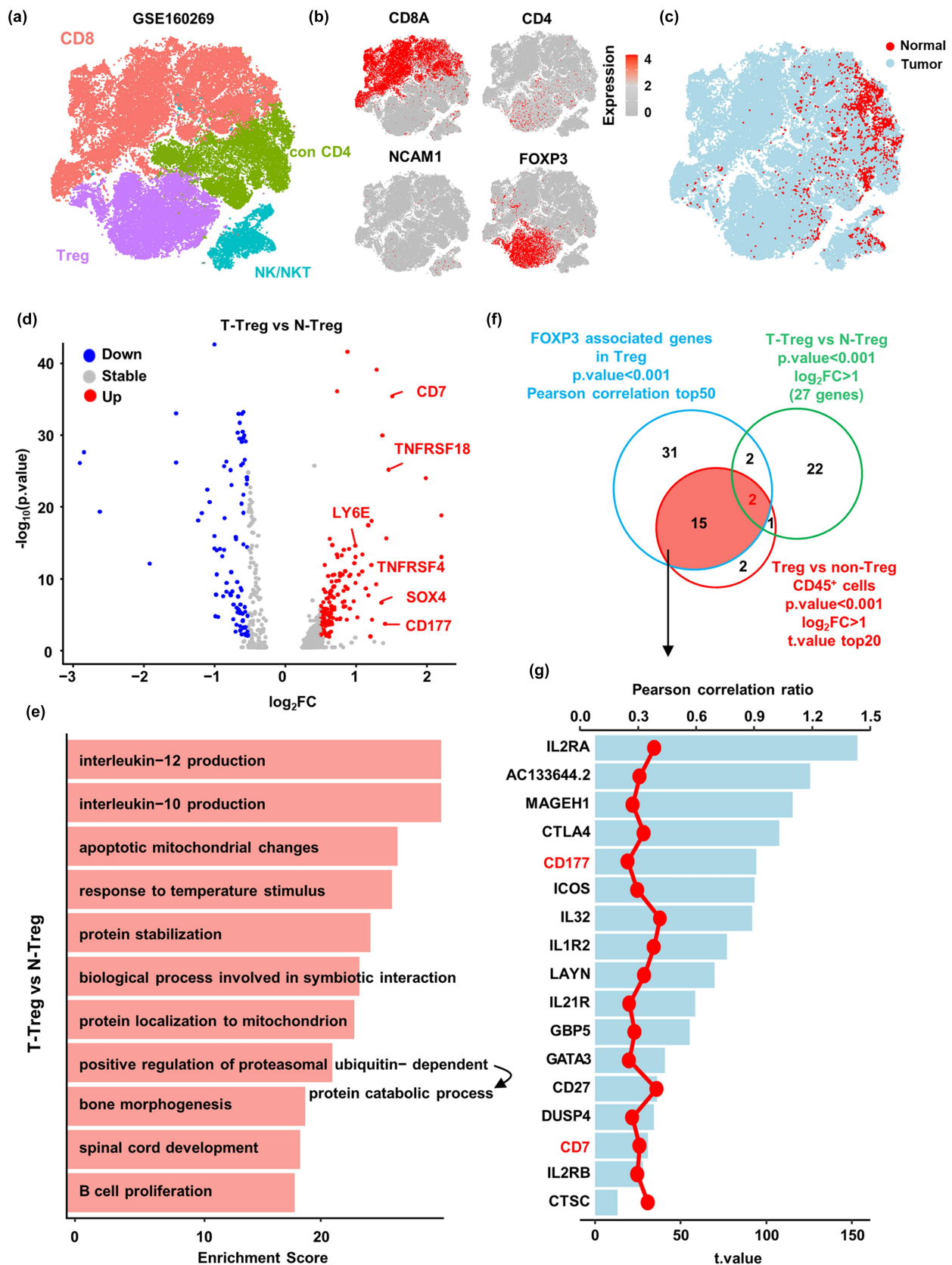


**Figure 1.** Characterization of tumor Treg-specific gene expression in ESCC. (a) Unsupervised t-SNE reduction plot of total T/NK cells in single-cell RNA sequencing data (GSE160269) containing ESCC tumor tissues (n = 60) and tumor-adjacent tissues (n = 4). (b) Feature plots of marker genes for T/NK-cell subset identification. (c) distribution of tumor- and tumor-adjacent tissue-derived T/NK cells in the t-SNE reduction plot. (d) Volcano plot of differentially expressed genes between T-Treg and N-Treg cells. Genes with a  $p$  value  $\leq 0.05$  and  $\log_2$  (fold change) in expression  $\geq 0.5$  (red) or  $\leq 0.5$  (blue) in T-Tregs vs. N-Tregs are highlighted and enumerated. (e) GO pathways of enriched genes upregulated in T-Treg cells and ranked by the enrichment score. (f) Venn plot of different gene sets: top 20 Treg-specific genes compared with non-Treg leukocytes (red), top 50 genes correlating with FOXP3 expression in Treg cells (blue), and upregulated genes by T-Treg cells compared with N-Treg cells (green). Seventeen genes overlapped between FOXP3-associated genes and Treg cell-specific genes (red fill), and two genes overlapped between three gene sets (red font). (g) A bar chart showing 17 overlapping genes between FOXP3-associated genes and Treg cell-specific genes in (F) ranked by the  $t$  value of Treg-specific genes (bottom axis). The line chart indicates Pearson's correlation ratio of these 17 genes with FOXP3 (top axis). Genes in red font overlapped between the three gene sets in (F).

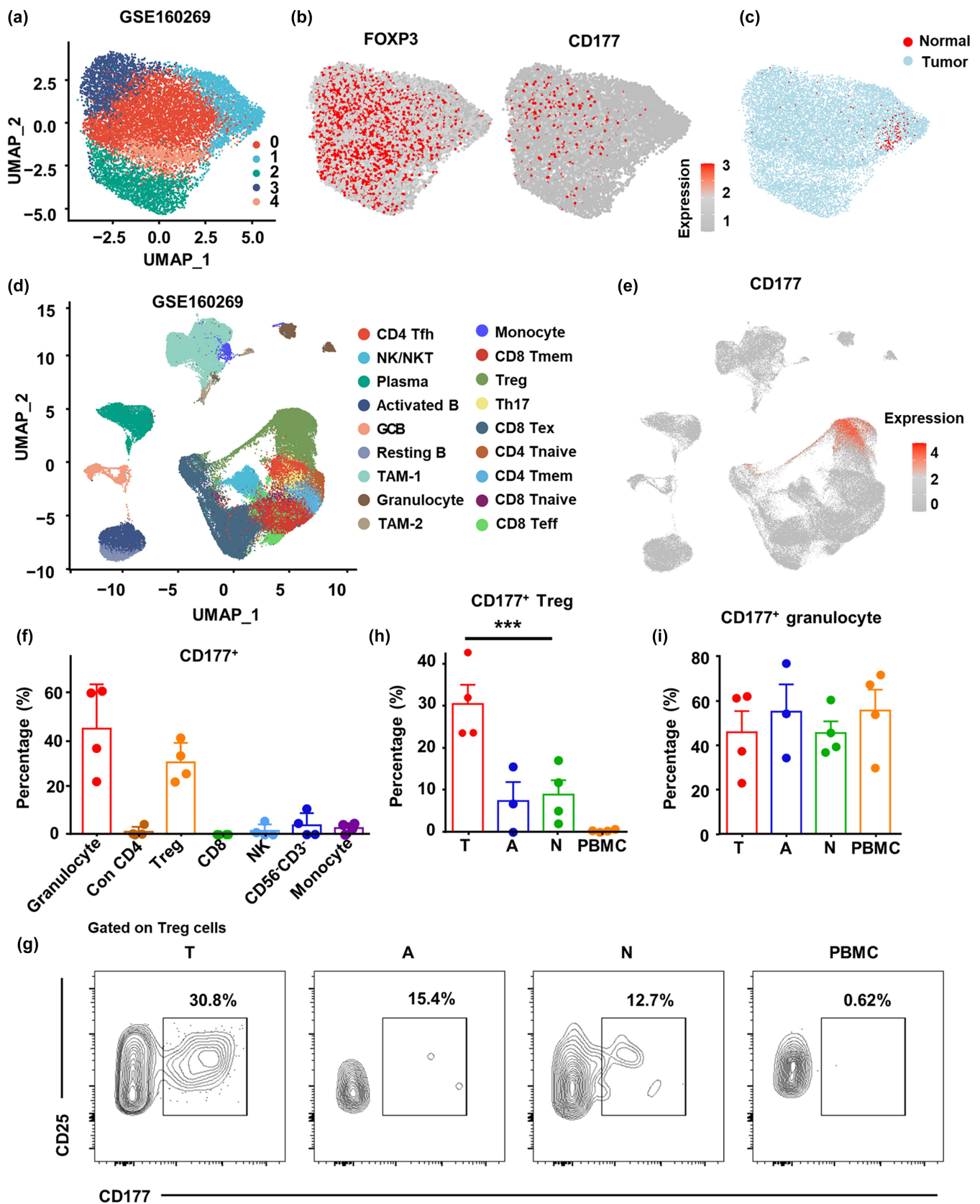


**Figure 2.** CD177 marks a unique Treg cell subset enriched in ESCC tumor tissue. (a) Unsupervised UMAP reduction plot of Treg cells in single-cell RNA sequencing data (GSE160269) containing ESCC tumor tissues ( $n = 60$ ) and tumor-adjacent tissues ( $n = 4$ ). (b) Feature plot of FOXP3 and CD177 expression in Treg cells. (c) Distribution of tumor- and tumor-adjacent tissue-derived Treg cells in the UMAP reduction plot. (d) Unsupervised UMAP reduction plot of total CD45-positive cells and cell subsets. TAM, tumor associated macrophage; Tmem, memory T; Tnaive, naive T; teff, effector T; Tex, exhausted T; Th17, T helper 17. (e) CD177 expression profile in total CD45-positive cells from ESCC tissues and tumor-adjacent tissues. (f) Flow cytometry data of CD177-positive cells among different immune cell subsets from ESCC tumor tissues ( $n = 4$ ). Con CD4, non-Treg conventional CD4<sup>+</sup> T. (g) Representative flow cytometry data and (H) statistical analysis of CD177<sup>+</sup> Treg cells from tumor tissues, tumor-adjacent tissues, normal esophagus tissues and PBMCs ( $n = 4$ ). (I) Statistical analysis of CD177<sup>+</sup> granulocytes from tumor tissues, tumor adjacent tissues, normal esophagus tissues and PBMCs ( $n = 4$ ). \*\*\* $p < 0.001$ , Student's t test.

PD-1 (Figure 3a, 2b). Flow cytometry analysis of tumor Treg cells revealed the same result (Figure 3b). To further explore the gene expression pattern of CD177<sup>+</sup> and PD-1<sup>+</sup> T-Treg cells, we performed semi-supervised clustering of Treg cells using ESCC scRNA-seq data (Figure 3C, supplementary table S3). We found that expression of PD-1 and CD177 was indeed mutually exclusive in T-Treg cells and that Treg cells could be divided into CD177<sup>+</sup> Treg, PD-1<sup>+</sup> Treg and double-negative (DN) Treg cells (Figure 3c,d). We then performed GO analysis to compare gene expression in these three Treg subsets (Figure 3e). We found that DN Treg cells expressed genes enriched in pathways associated with dendritic cell antigen presentation and dendritic cell migration, indicating that DN Treg cells may be the precursor activated Treg cells. PD-1<sup>+</sup> Treg cells were found to express genes enriched in pathways related to cytolysis, pyroptosis and apoptosis. Genes associated with the T-cell tolerance induction pathway were upregulated in CD177<sup>+</sup> Treg cells, indicating that they have a high suppressive function in the ESCC tumor microenvironment (Figure 3e). Interestingly, CD177<sup>+</sup> Treg cells were also shown to express genes associated with cell shape changes and cytoskeleton remodeling (Figure 3e), suggesting that CD177 might regulate Treg cell migration, as reported for neutrophils. However, CD177<sup>+</sup> Treg cells do not express other receptors that can interact with CD177 in neutrophils, such as ITGAM (CD11b coding gene), and FCGR1IB (CD16b coding gene) (Fig. S2H). Three subsets of Treg cells constitutively express the CD18 coding gene ITGB1 (Fig. S2H).

We further compared expression of genes directly related to Treg function and found that CD177<sup>+</sup> Treg cells highly express CTLA4 and TNFRSF4, which are involved in the Treg suppressive function and survival in the tumor microenvironment (Figure 3F). They highly express the suppressive molecule TGF- $\beta$  encoded by TGFB2. CD177<sup>+</sup> Treg cells also express the previously reported tumor Treg marker CCR8, however CCR8 is also expressed in PD-1<sup>+</sup> cells and DN Treg cells (Fig. S2I). Moreover, CD177<sup>+</sup> Treg cells were shown to express high levels of EBI3, a subunit of IL-35. Treg cell-derived IL-35 is important in inducing inhibitory receptor expression on T cells and limiting central memory T-cell differentiation, whereas Treg cell-derived IL-10 participates in directly suppressing T-cell activation.<sup>40</sup> These results suggest that CD177<sup>+</sup> Treg and PD-1<sup>+</sup> Treg cells might perform suppressive functions in the tumor microenvironment through different mechanisms. Moreover, we found that EBI3 expression correlated positively with the CD177<sup>+</sup> Treg cell infiltration score in ESCC microarray data (GSE53625) (Figure 3g) but negatively with the PD-1<sup>+</sup> Treg infiltration score in ESCC tumor tissue (Fig. S3A). EBI3 expression did not correlate with the DN Treg infiltration score (Fig. S3A). Ex vivo stimulation of sorted three Treg cell clusters demonstrated that CD177<sup>+</sup> Treg cells exhibit high ability to secrete IL-35, while PD-1<sup>+</sup> Treg cells show elevated secretion of IL-10 (Figure 3h). The segregated expression of IL-10 and IL-35 in tumor Treg cells are consistent with a previous report.<sup>40</sup> These results suggest that CD177<sup>+</sup> Treg cells is the major source of IL-35 while PD-1<sup>+</sup> Treg cells is the major source of IL-10 in ESCC.

By analyzing ESCC scRNA-seq data, we also found that CD177<sup>+</sup> Treg cells correlated positively with exhausted CD8<sup>+</sup>

T cells and negatively with Th17 cells, which are involved in antitumor immunity (Figure 3i). Meanwhile, CD177<sup>+</sup> Treg correlated negatively with germinal center B cells (GCBs) and T follicular helper (Tfh) cells (Figure 3i). GCB and Tfh cells are vital components for tertiary lymphatic structure (TLS) formation, and they play an important role in tumor eradication.<sup>41</sup> However, the percentage of DN Treg cells correlated positively with resting B cells and negatively with exhausted CD8<sup>+</sup> T cells (Fig. S3B). The percentage of PD-1<sup>+</sup> Treg cells correlated positively with Th17, GCB cells and effector CD8<sup>+</sup> T cells (Fig. S3B). These results suggest that CD177<sup>+</sup> Treg cells represent a distinct Treg cell subset from PD-1<sup>+</sup> Treg cells in tumor microenvironment and might perform their suppressive function through IL-35 expression.

### Pan-cancer analysis reveals different developmental trajectories of CD177<sup>+</sup> and PD-1<sup>+</sup> Treg cells

We utilized a pan-cancer scRNA-seq data (GSE156728) to explore the developmental relationship between CD177<sup>+</sup> Treg and PD-1<sup>+</sup> Treg cells<sup>42</sup> and performed semi-supervised clustering (Supplementary table S3). Consistent with our findings in ESCC, we found expressions of CD177 and PD-1 to be mutually exclusive in Treg cells from many tumor types, and similarly, we clustered them into three groups (Figure 4a,b). The differential gene heatmap showed that DN Tregs express the naïve T-cell marker CCR7 and that CD177<sup>+</sup> Treg cells highly express CCR8, O $\times$ 40 and GITR (Figure 4c). In contrast, PD-1<sup>+</sup> Treg cells exhibited increased expression of LAG3, which supports their exhausted state. We then performed TCR repertoire clonotype analysis and found that CD177<sup>+</sup> Treg cells exhibited enhanced clonal expansion compared to PD-1<sup>+</sup> Treg cells and DN Treg cells (Figure 4d). Although previous evidence suggests that PD-1<sup>+</sup> Treg cells undergo clonal expansion during tumor progression,<sup>43</sup> our data revealed a unique Treg cell subset that is more clonally expanded than PD-1<sup>+</sup> Treg cells. Common TCR clonotype analysis indicated that the CD177<sup>+</sup> Treg cells share partial common TCR clones with PD-1<sup>+</sup> Treg cells despite the unique clonotypes (Figure 4e). To understand the developmental trajectory of these three Treg cell subsets, we conducted pseudotime reduction analysis and found that the developmental trajectory derived from DN Tregs diverged into two different branches from a certain node and pointed at CD177<sup>+</sup> Treg and PD-1<sup>+</sup> Treg respectively (Figure 4f). Thus, CD177<sup>+</sup> Treg and PD-1<sup>+</sup> Treg might develop from the same origin. In summary, we found a unique CD177<sup>+</sup> Treg cell subset with enhanced clonal expansion and different developmental trajectories and functions from PD-1<sup>+</sup> Treg cells in the tumor microenvironment.

### Higher CD177<sup>+</sup> Treg cell infiltration is associated with poor survival in ESCC patients

We then sought to determine whether CD177<sup>+</sup> Treg cells are associated with clinical prognosis of ESCC patients. scRNA-seq data showed that tumors at late stages had a higher CD177<sup>+</sup> Treg cell percentage (Figure 5a). By using the Cibersort algorithm, we predicted the CD177<sup>+</sup> Treg cell score, as well as PD-1<sup>+</sup> and DN Treg cell scores of ESCC tissue from microarray data (GSE53625) (Figure 5b, Fig. S4A). We found that CD177<sup>+</sup>

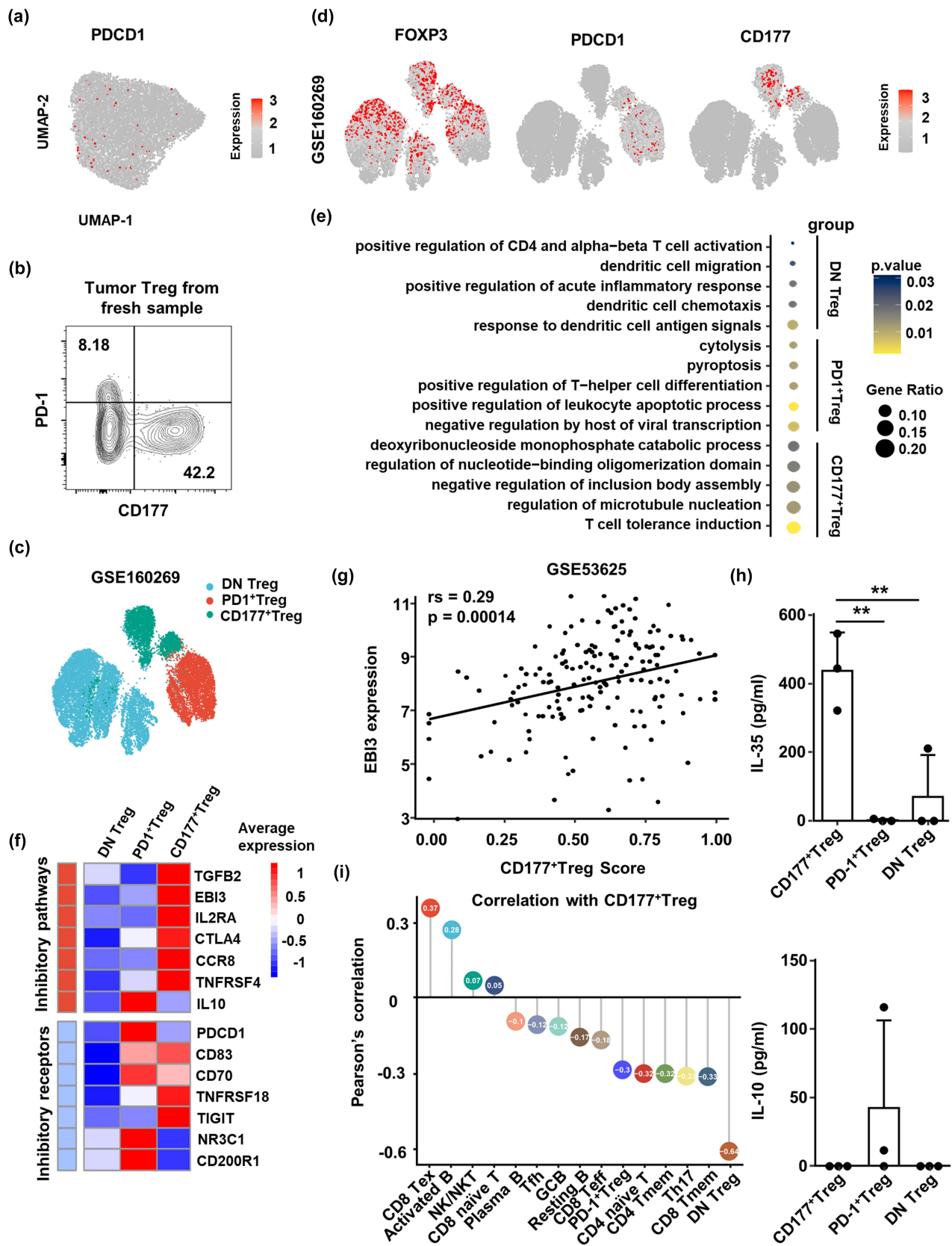


**Figure 3.** PD-1<sup>+</sup> and CD177<sup>+</sup> Treg cells represent two distinct Treg cell subsets in ESCC. (a) Unsupervised UMAP reduction plot of PDCD1 expression profile in Treg cells from ESCC. (b) Representative flow cytometry results of CD177 and PD-1 expression patterns on tumor Treg cells (CD45<sup>+</sup>CD3<sup>+</sup>CD56<sup>-</sup>CD4<sup>+</sup>CD127<sup>-</sup>CD25<sup>+</sup>). (c) Semi-supervised UMAP reduction plot of Treg cells in single-cell RNA sequencing data containing ESCC tumor tissues ( $n = 60$ ) and tumor-adjacent tissues ( $n = 4$ ). Treg cells were divided into three subsets according to PDCD1 and CD177 expression. (d) Feature plots showing expression patterns of FOXP3, PDCD1 and CD177 in Treg cells. (e) Top five enriched GO pathways of genes expressed by the three Treg subsets. (f) Heatmap showing the expression pattern of genes from two Treg function-associated gene sets by the three Treg cell subsets. (g) Spearman's correlation analysis between the CD177<sup>+</sup> Treg score and EB13 in ESCC microarray data (GSE53625), Spearman's correlation coefficient was shown as  $rs$ . (h) 4,000 CD177<sup>+</sup>, PD-1<sup>+</sup>, or DN Treg cells from the tumor and tumor-adjacent tissues were sorted and stimulated ex vivo with human anti-CD3 (2  $\mu$ g/ml), anti-CD28 (1  $\mu$ g/ml) and rIL-2 (50 U/ml) in a 96-well round bottom plate respectively. After 72 hours, the supernatants were collected for ELISA analysis of IL-10 and IL-35. (i) Pearson's correlation analysis between the CD177<sup>+</sup> Treg cell percentage and the percentages of different immune cell types from ESCC single-cell RNA sequencing data.



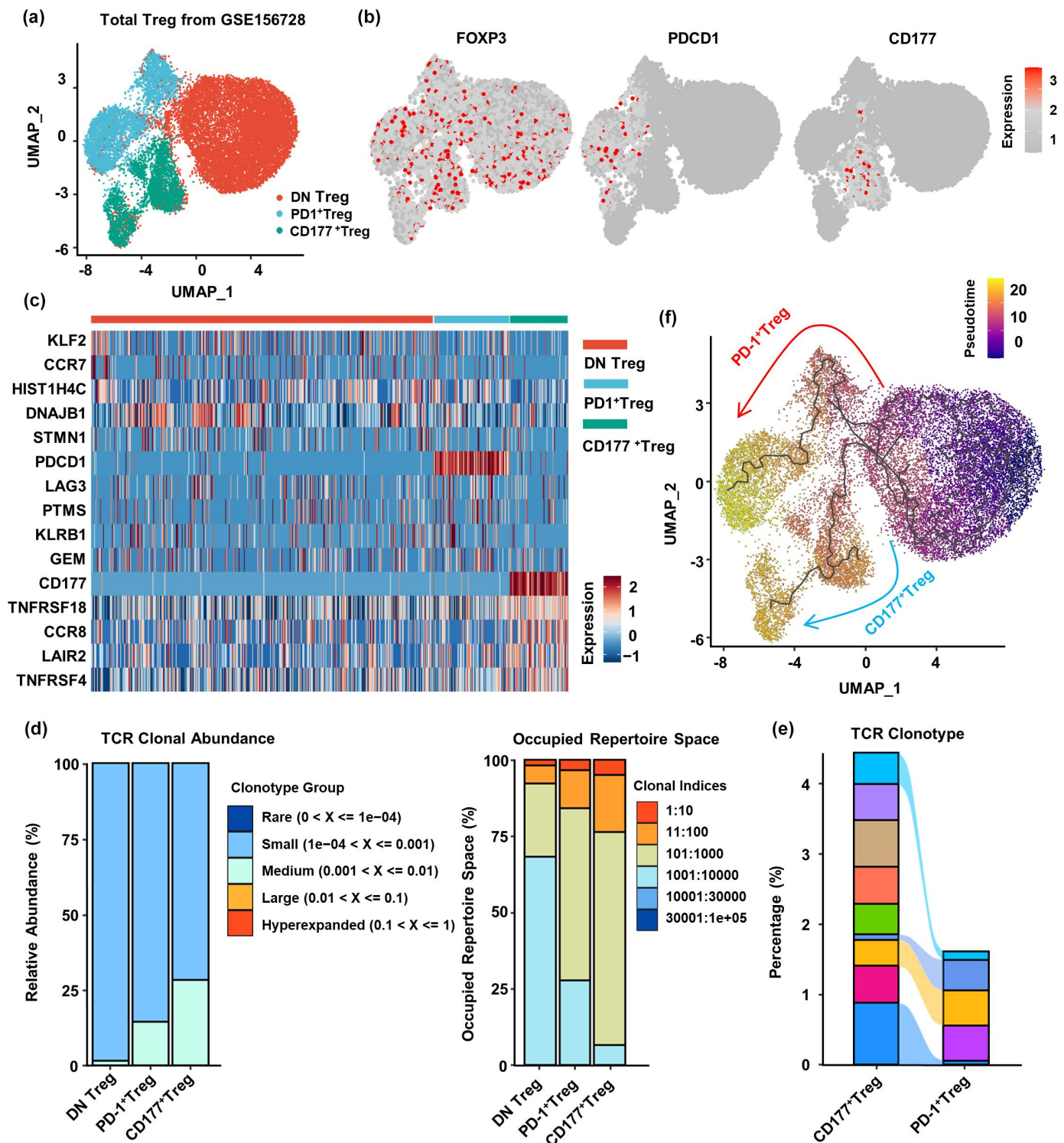


**Figure 4.** Pan-cancer analysis reveals different developmental trajectories of CD177<sup>+</sup> and PD-1<sup>+</sup> tumor Treg cells. (a) Semi-supervised UMAP reduction plot of Treg cells from single-cell RNA sequencing data of pan-cancer tumor tissues and tumor-adjacent tissues (GSE156728). (b) Feature plots showing expression patterns of FOXP3, PDCD1 and CD177 in Treg cells. (c) Heatmap showing the top five differentially expressed genes in the three Treg cell subsets. (d) TCR repertoire abundance and occupied repertoire space of the three Treg cell subsets. (e) Sankey chart displaying the top 10 abundant TCR clonotypes of CD177<sup>+</sup> Treg and PD-1<sup>+</sup> Treg cells and potential common clonotypes between these two subsets. (f) Pseudotime trajectory analysis of pan-cancer Treg cells showing two different developmental trajectories of CD177<sup>+</sup> Treg and PD-1<sup>+</sup> Treg cells from DN Treg cells.

Treg and DN Treg cells were enriched in the tumor compared with normal tissue (Figure 5b), while no enrichment was observed in PD-1<sup>+</sup> Treg cells (Fig. S4A). Patients were divided according to the CD177<sup>+</sup> Treg score into CD177<sup>+</sup>Treg<sup>hi</sup> and CD177<sup>+</sup>Treg<sup>lo</sup> cohorts, with those in the former displaying

decreased overall survival probability (Figure 5c). However, there were no differences in overall survival probability between PD-1<sup>+</sup>Treg<sup>hi</sup> and PD-1<sup>+</sup>Treg<sup>lo</sup> cohorts, as well as DN Treg<sup>hi</sup> and DN Treg<sup>lo</sup> cohorts (Fig. S4B). We then analyzed additional proteomic data (PXD021701)<sup>31</sup> and found similar

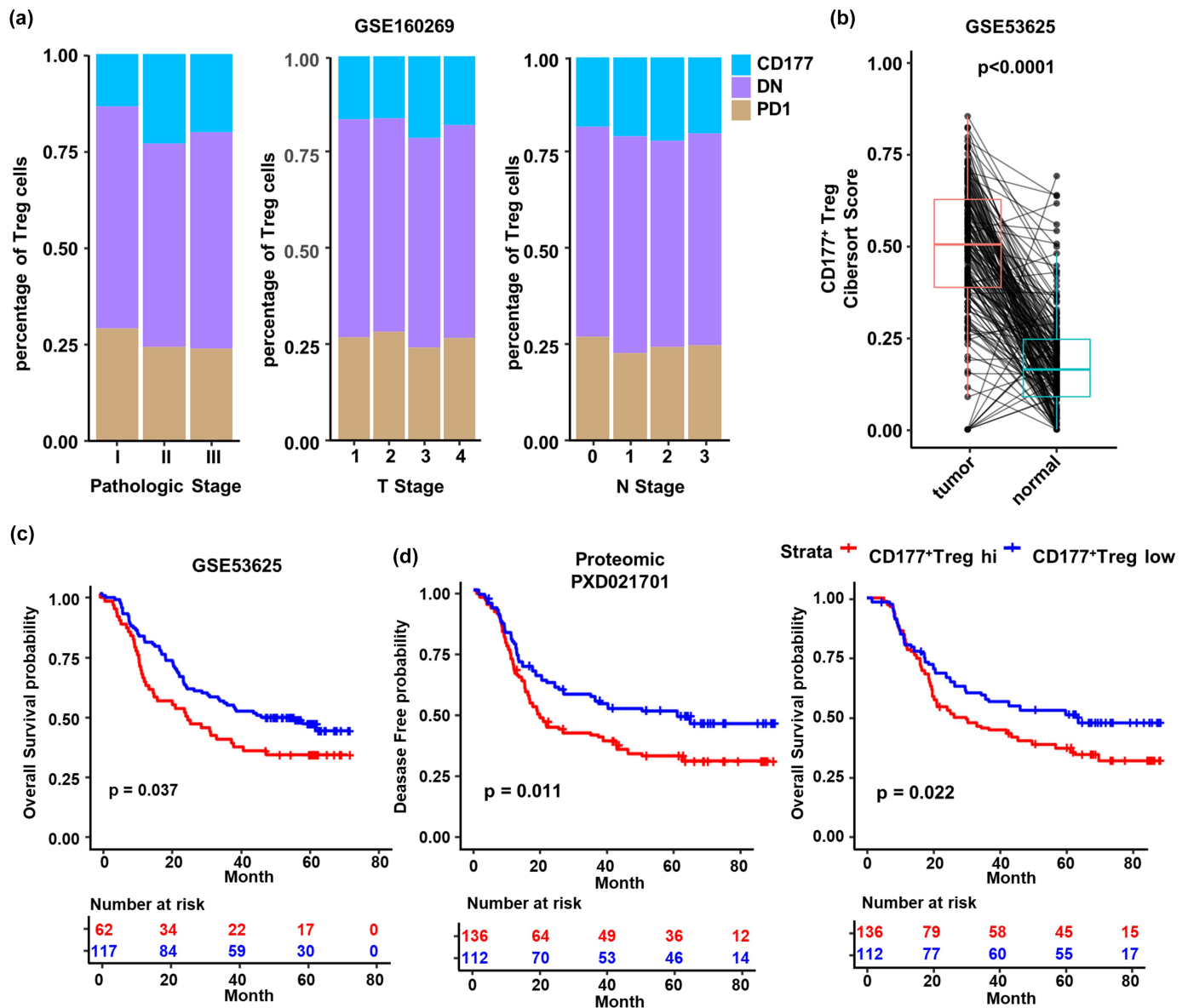


**Figure 5.** Higher CD177<sup>+</sup> Treg cell infiltration is associated with poor survival of ESCC patients. (a) Analysis of compositions of the three Treg cell subsets in tumors from patients with different pathologic stages, T stages and N stages in ESCC single-cell RNA sequencing data (GSE160269). (b) Predicted CD177<sup>+</sup> Treg cell score of tumor tissues and normal tissues using Cibersort from ESCC microarray data (GSE53625). (c) Overall survival probability of ESCC patients with high or low CD177<sup>+</sup> Treg cell score from the GSE53625 cohort. (d) Disease-free probability and overall survival probability of ESCC patients with high or low CD177<sup>+</sup> Treg cell scores based on proteomic data from another cohort (PXD021701). *p* value was calculated using Kaplan – Meier (log rank) test.

results: patients in the CD177<sup>+</sup> Treg<sup>hi</sup> cohort had decreased disease-free probability and overall survival probability (Figure 5d). Therefore, we found that the accumulation of CD177<sup>+</sup> Treg cells is an indicator of poor prognosis in ESCC.

### Anti-PD-1 immunotherapy impairs CD177<sup>+</sup> Treg cells and boosts PD-1<sup>+</sup> Treg cells in ESCC

CD177 and PD-1 are mutually exclusively expressed on Treg cells, however, a low percentage of PD-1<sup>+</sup> Treg cells were observed by flow cytometry in untreated tumor tissue (Figure 2b). As PD-1<sup>+</sup> Treg cells are associated with the efficacy of anti-PD-1 immunotherapy in many tumors, we wondered if CD177<sup>+</sup> Treg cells also play a role in this process. We found that the CD177<sup>+</sup> Treg cell frequency decreased while the PD-1<sup>+</sup> Treg cell frequency increased in tumor tissue from patients after

neoadjuvant anti-PD-1 immunotherapy compared with untreated patients (Figure 6(a-c)). This was observed only in tumor tissue and not in tumor-adjacent tissue, normal esophageal tissue or peripheral blood (Figure 6b,c). To further investigate the Treg subset spatial distribution in ESCC, we conducted mIHC staining of tumor tissues from 19 untreated ESCC patients and 21 ESCC patients who underwent neoadjuvant anti-PD-1 immunotherapy with stable disease (SD) and partial response (PR). We did not observe CD177 and PD-1 double-positive Treg cells in all tissues, and tumor tissues exhibited a significantly higher CD177<sup>+</sup> Treg cell percentage (Figure 6d, e), consistent with our flow cytometry and scRNA-seq results. Treg cell infiltration was increased in tumor-adjacent tissue from patients underwent anti-PD-1 immunotherapy, while most Treg cells do not express CD177 (Figure 6d). And, we also identified CD177<sup>+</sup> non-Treg cells which exhibited the characteristic lobed

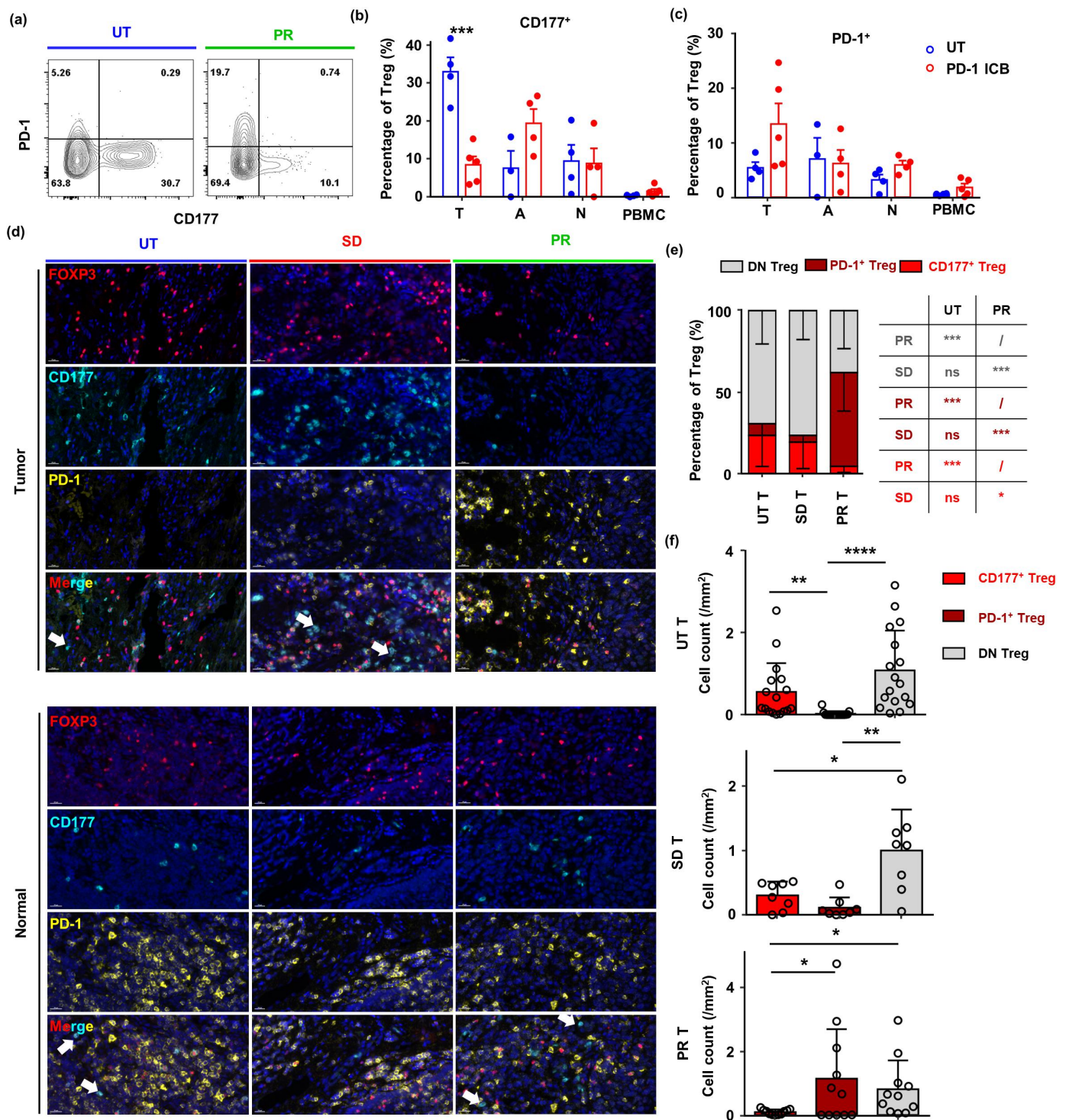


**Figure 6.** Anti-PD-1 immunotherapy impairs CD177<sup>+</sup> Treg and boosts PD-1<sup>+</sup> Treg cells in ESCC. (a) Representative flow cytometry result of CD177 and PD-1 expression by tumor Treg cells from surgical samples of untreated patients and patients with a partial response to neoadjuvant anti-PD-1 immunotherapy plus chemotherapy. (b) Statistical analysis of CD177<sup>+</sup> Treg cell percentages in tumor tissues, tumor-adjacent tissues, normal esophagus tissues and PBMCs from untreated patients (n = 4) and patients treated with neoadjuvant anti-PD-1 immunotherapy plus chemotherapy (n = 5). (c) Statistical analysis of PD-1<sup>+</sup> Treg cell percentages in tumor tissues, tumor-adjacent tissues, normal esophagus tissues and PBMCs from untreated patients (n = 4) and patients treated with neoadjuvant anti-PD-1 immunotherapy plus chemotherapy (n = 5). (d) Multiplexed immunohistochemistry staining of tumor tissues and tumor-adjacent tissues from untreated patients and patients with PR and SD after neoadjuvant anti-PD-1 immunotherapy plus chemotherapy. White arrows indicate CD177<sup>+</sup> non-Treg cells which may be granulocytes. (e) Statistical analysis of percentages of different Treg cell subsets in tumor (T) from untreated patients (n = 19) and patients with PR (n = 12) and SD (n = 9) after neoadjuvant anti-PD-1 immunotherapy plus chemotherapy. (f) Cell density of three Treg cell subsets in tumor tissue of ESCC patients among different cohorts, UT, PR and SD. Statistical analysis was performed using Student's t-test. \**p* < 0.05, \*\**p* < 0.01, \*\*\**p* < 0.001.

nuclear morphology as granulocytes (Figure 6d). Interestingly, the percentage of CD177<sup>+</sup> Treg cells rather than PD-1<sup>+</sup> Treg cells decreased in patients underwent anti-PD-1 immunotherapy and was lower in PR patients than in SD patients (Figure 6e). We calculated the density of the three Treg cells per unit area and obtained similar results (Figure 6f). Besides, we also observed decreased CD177<sup>+</sup>Treg cells after anti-PD-1 treatment in oral cancer, while the frequencies of PD-1<sup>+</sup> and DN Treg cells were not affected (Fig. S4C-D). These results indicate that CD177<sup>+</sup>Treg cells may be associated with poor response to ESCC neoadjuvant anti-PD-1 immunotherapy.

### Lymphatic endothelial cells are associated with CD177<sup>+</sup> Treg accumulation in tumor tissue in ESCC

We then explored how CD177<sup>+</sup> Treg cells accumulate in ESCC tumor tissue. The reported ligand for CD177 is CD31, which is expressed by endothelial cells and regulates CD177<sup>+</sup> neutrophil adherence and residency.<sup>35,44</sup> We found that CD31 did co-localize with CD177<sup>+</sup> Treg cells in ESCC tumor tissue from untreated patients (Fig. S5A). ScRNA-seq data analysis identified that the CD31 encoding gene PECAM1 was only expressed by endothelial cells and lymphatic endothelial cells (LECs) (Figure 7a, Fig. S5B-C). We then performed correlation analysis and found that CD177<sup>+</sup> Treg cells correlated positively with CD31<sup>+</sup> LECs, with no correlation detected with CD31<sup>+</sup> endothelial cells (Figure 7b). Moreover, mIHC results showed that CD177<sup>+</sup> Treg cells have closer spatial distance with LYVE1<sup>+</sup> LECs compared to PD-1<sup>+</sup> and DN Treg cells in ESCC tumor tissue (Figure 7c,d). The density of LECs decreased in patients that partially response to anti-PD-1 immunotherapy plus chemotherapy, compared to patients with stable disease and untreated patients (Figure 7(c-e)). Moreover, LEC density positively correlated with the percentage of CD177<sup>+</sup> Treg cells, while negatively correlated with PD-1<sup>+</sup> Treg cells (Fig. S5D). No correlation was observed between LEC density and the percentage of DN Treg cells. Furthermore, we performed in vitro co-cultured LECs with tumor-infiltrating Tregs. By flipping the culture dish to remove cells that could not adhere to the LECs, we found a significant enrichment in the percentage of CD177<sup>+</sup> Tregs (Figure 7f,g). Therefore, LECs are associated with CD177<sup>+</sup> Treg cell accumulation in ESCC tumor tissue and patients' response to anti-PD-1 immunotherapy and chemotherapy.

### Discussion

In this study, we characterized tumor-infiltrating Treg cells using scRNA-seq data, and by combined analysis of Treg-associated genes, we identified CD177 as a tumor Treg cell marker in ESCC. Moreover, we found that CD177<sup>+</sup> Treg cell infiltration can serve as a prognostic marker for survival and response to anti-PD-1 immunotherapy in ESCC.

Human tumor-infiltrating Treg cells can be divided into three subsets based on FOXP3 and CD45RA expression, and only effector Treg (eTreg, FOXP3<sup>hi</sup>CD45RA<sup>-</sup>) cells have the strongest immunosuppressive activity and tumor antigen reactivity.<sup>6,45</sup> eTreg cells express high levels of PD-1 and

have a strong ability to produce immunosuppressive cytokines such as IL-10 and TGF- $\beta$ .<sup>40</sup> Many studies have also reported that PD-1<sup>+</sup> Treg cells are highly immunosuppressive and tumor antigen specific.<sup>6</sup> We initially hypothesized that Treg cells in ESCC also express high levels of PD-1. However, we found that only 3% of Treg cells expressed PD-1, with 30% expressing CD177. This revealed a distinct tumor microenvironment of ESCC and highlighted that CD177<sup>+</sup> Treg cells may be critical in suppressing antitumor immunity. It has been reported that CD177<sup>+</sup> Treg cells accumulate in renal clear cell carcinoma and display an effector Treg phenotype.<sup>36</sup> Additional evidence highlights CD177<sup>+</sup> Treg cell enrichment in lung cancer, colorectal cancer and melanoma.<sup>37</sup> However, the function and underlying mechanism of CD177<sup>+</sup> Treg cells in tumor progression need further investigation. Based on pan-cancer analysis, we found that CD177<sup>+</sup> Treg cells in ESCC, or in many tumor types, do not express PD-1. CD177<sup>+</sup> Treg cells display different gene expression profiles compared with PD-1<sup>+</sup> Treg cells, including increased coinhibitory molecule expression and enrichment of immunotolerance induction pathways. Moreover, CD177<sup>+</sup> Treg cells express high levels of CCR8, a marker of highly suppressive tumor-infiltrating Treg cells.<sup>46,47</sup> Interestingly, different from PD-1<sup>+</sup> Treg cells, which express a high level of IL10, CD177<sup>+</sup> Treg cells highly express immunosuppressive cytokine IL-35. Higher serum IL-35 levels indicate poor clinical prognosis and enhanced tumor progression in many cancer types.<sup>48</sup> Other evidence has demonstrated that Treg cell-derived IL-35 contributes to high levels of PD-1, TIM-3 and LAG-3 expression and functional exhaustion of tumor-infiltrating CD8<sup>+</sup> T cells.<sup>40</sup> Although anti-PD-1 antibodies effectively inhibit the negative immunomodulatory effects of the checkpoint molecule PD-1, the presence of other immune checkpoints like TIM-3 and LAG-3 may still mediate the suppressive functions of IL35 secreted by CD177<sup>+</sup> Tregs. This process is likely unaffected by anti-PD-1 immunotherapy. And that can explain why high CD177<sup>+</sup> Treg cell infiltration is associated not only with poor survival but also poor response to anti-PD-1 immunotherapy in ESCC patients. One of the reasons may be that CD177<sup>+</sup> Treg cells secreted IL-35 can induce expression of other co-inhibitory molecules and thus exhaustion of tumor infiltrating CD8<sup>+</sup> T cells, even when PD-1/PD-L1 interaction is blocked by anti-PD-1 immunotherapy. Our work revealed that PD-1<sup>+</sup> and CD177<sup>+</sup> Treg cells may cooperate in creating a suppressive tumor immune microenvironment and highlights that CD177<sup>+</sup> Treg cell infiltration is an important factor to consider in anti-PD-1/PD-L1 immunotherapies.

The mechanism by which CD177<sup>+</sup> Treg cells accumulate in the tumor microenvironment remains unknown. Our data suggest that CD177 assists in Treg accumulation through binding of its ligand CD31 in LECs. LECs play dual roles in tumor immunity and immunotherapy response.<sup>49</sup> They transport tumor antigens for lymphocyte priming and also express immune-inhibitory molecules to create an immunosuppressive microenvironment. The CD177 and CD31 axis might be a key signaling pathway of LEC recruitment of CD177<sup>+</sup> Treg cells. Besides, LEC derived CD31 signal may not only maintain CD177<sup>+</sup> Treg residency in situ but also rise more opportunity

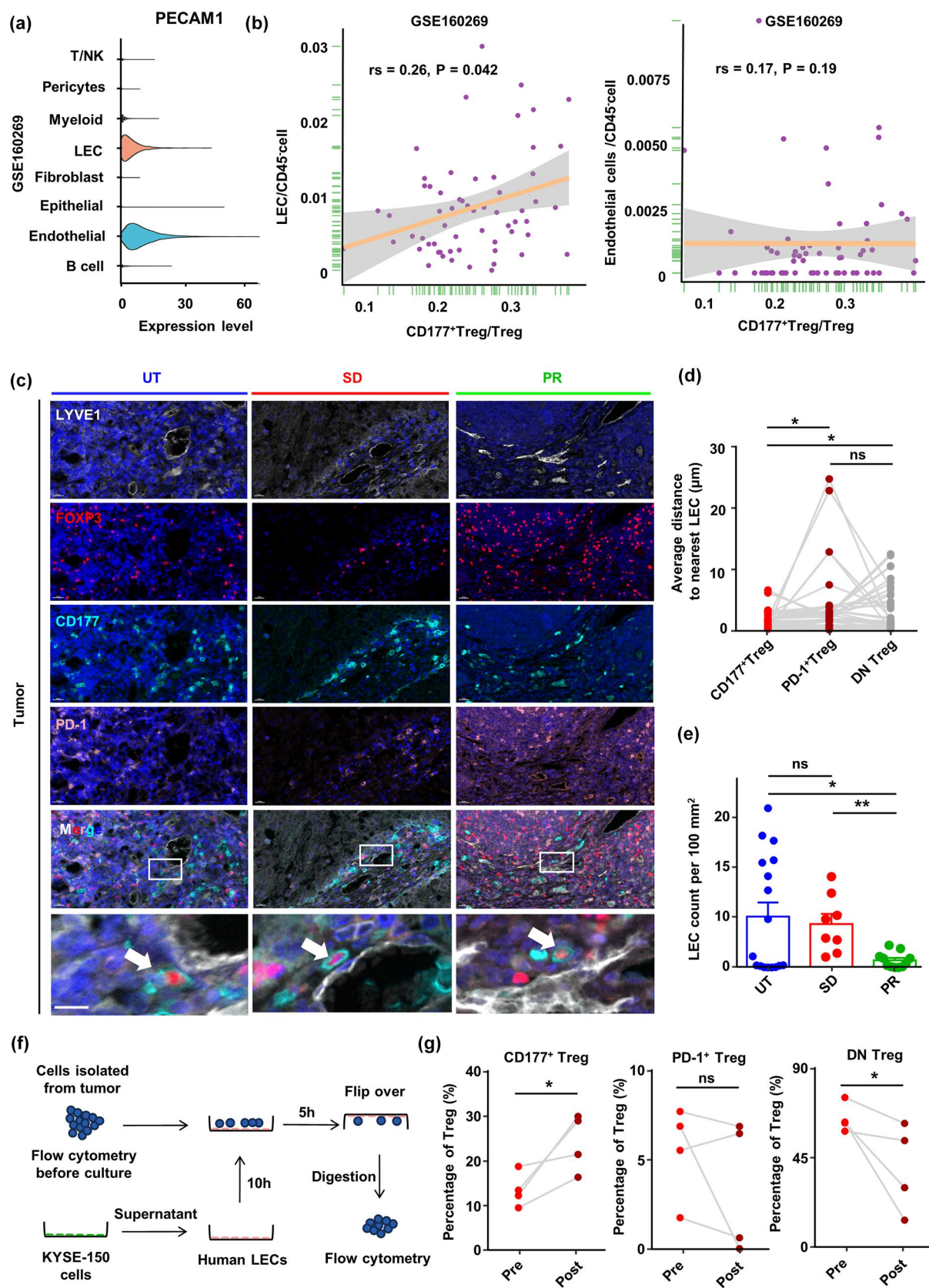


**Figure 7.** CD31 expression by lymphatic endothelial cells is associated with CD177<sup>+</sup> Treg cell accumulation in tumor tissue in ESCC. (a) Expression of the CD177 ligand PECAM1 (CD31) by different cell subsets in ESCC single-cell RNA sequencing data (GSE160269). (b) Spearman's correlation analysis of the percentage of LECs and endothelial cells and CD177<sup>+</sup> Treg cells from ESCC single-cell RNA sequencing data (GSE160269). Spearman's correlation coefficient was shown as rs. (c) IHC staining of LYVE1, CD177, PD-1, and FOXP3 in tumor tissue from UT (n = 17), SD (n = 8) and PR (n = 11) ESCC patients. (d) Statistical analysis of average distance between three Treg cell subsets and nearest LEC in tumor tissues of all patients (n = 36). Statistical analysis was performed using a paired Student's t-test. (e) Statistical analysis of LEC density between UT (n = 17), SD (n = 8) and PR (n = 11) tumor tissues. (f) Adhesion assay strategy: cells were isolated from tumor and adjacent non-cancerous tissues and tested with flow cytometry to evaluate the proportions of the three Treg cell groups before co-culture. Subsequently, these cells are co-cultured for 5 hours with human primary LECs that have been pre-treated with supernatant from the ESCC tumor cell line KYSE-150. Afterward, the culture dish is flipped over, remaining cells are digested with 0.25% trypsin for flow cytometry analysis. (g) Bar chart showing the change in proportions of the three Treg cell groups before and after the adhesion assay experiment. Statistical analysis was performed using an unpaired or paired Student's t-test. \* $p < 0.05$ , \*\* $p < 0.01$ , \*\*\* $p < 0.001$ .

of tumor antigen exposure. This might account for the higher clonal expansion of CD177<sup>+</sup> Treg cells over PD-1<sup>+</sup> and DN Treg cells. Importantly, we found that LEC density in tumor tissue decreased after anti-PD-1 immunotherapy plus chemotherapy. Thus, blocking LEC-derived CD31 signaling combined with anti-PD-1 immunotherapy may benefit patients who do not respond to other therapies.

The function of CD177 is still poorly understood. In neutrophils, CD177 binds to its ligand CD31 on endothelial cells and facilitates transendothelial migration, mainly through decreasing endothelial cell junctional integrity.<sup>50</sup> However, ligation of CD177 resulted in activation of integrin CD11b/CD18 signal and inhibited chemokine mediated migration of neutrophils.<sup>35</sup> CD177 can suppress Wnt/ $\beta$ -catenin signaling pathway to limit tumor progression. A previous study reported that anti-CD177 blocking antibody or CD177 knockout can abrogate the suppressive function of CD177<sup>+</sup> Treg cells in vitro,<sup>36</sup> suggesting that CD177 can intrinsically modulate Treg cell function, but the mechanism remains unknown. As CD177 do not have a signal transduction domain, it may transduce signal through interaction with other receptors such as CD11b and CD18. We found that tumor Treg cells in ESCC do not express ITGAM, but constitutively express ITGB2, which encodes CD18. CD18 is reported to be important in Treg cell development and lineage stability.<sup>51,52</sup> Whether CD18 participated in CD177-CD31 regulated Treg cell function in tumor microenvironment of ESCC needs further investigation.

## List of abbreviations

DN	double negative
ESCC	esophageal squamous cell carcinoma
eTreg	effector regulatory T cell
GCB cell	germinal center B cell
GO	gene ontology
LEC	lymphatic endothelial cell
mIHC	multiplexed immunohistochemistry
N-Treg	tumor-adjacent Treg
PR	partial response
scRNA-seq	single-cell RNA sequencing
SD	stable disease
TCR	T cell receptor
Tfh cell	T follicular helper cell
TLS	tertiary lymphoid structure
t-SNE	t-distributed stochastic neighbor embedding
T-Treg	tumor-infiltrating Treg
UMAP	uniform manifold approximation and projection

## Disclosure statement

No potential conflict of interest was reported by the author(s).

## Funding

The work was supported by the National Natural Science Foundation of China [82173083]; Natural Science Foundation of Guangdong Province [2022A1515012469]; the Program for Guangdong Introducing Innovative and Entrepreneurial Teams [2017ZT07S054]; State Key Laboratory of Pathogenesis, Prevention, Treatment of Central Asian High Incidence Diseases Fund, China [SKL-HIDCA-2021-7]; Science and Technology Program of Guangzhou, China [202206010103].

## ORCID

Liang Li  <http://orcid.org/0000-0003-0745-2571>  
Zhe-Xiong Lian  <http://orcid.org/0000-0002-9525-1421>

## Author contributions

Z.X. Lian, G. Qiao, L. Li, and S.H. Yang designed the project. M. Ma, C. Huang and S.H. Yang performed the flow cytometry and immunohistochemistry experiments and analyzed the data. M. Ma and L. Li analyzed the single-cell RNA sequencing, microarray, and proteome mass spectrometry data. W. Zhuang, S. Huang, X. Xia, Y. Tang, Z. Li, X. Ben and G. Qiao provided human samples and patients' information. M. Ma and L. Li wrote the manuscript, other authors revised the manuscript.

## Data availability statement

All data generated in this manuscript will be provided upon request to corresponding authors.

## References

- Lu CL, Lang H-C, Luo J-C, Liu C-C, Lin H-C, Chang F-Y, Lee S-D. Increasing trend of the incidence of esophageal squamous cell carcinoma, but not adenocarcinoma, in Taiwan. *Cancer Causes Control.* 2010;21(2):269–274. doi:10.1007/s10552-009-9458-0.
- Zheng S, Liu B, Guan X. The role of tumor microenvironment in invasion and metastasis of esophageal squamous cell carcinoma. *Front Oncol.* 2022;12:911285. doi:10.3389/fonc.2022.911285.
- Vinay DS, Ryan EP, Pawelec G, Talib WH, Stagg J, Elkord E, Lichter T, Decker WK, Whelan RL, Kumara HMCS. et al. Immune evasion in cancer: mechanistic basis and therapeutic strategies. *Semin Cancer Biol.* 2015;35:S185–S198. doi:10.1016/j.semcancer.2015.03.004.
- Wing JB, Tanaka A, Sakaguchi S. Human FOXP3(+) regulatory T cell heterogeneity and function in autoimmunity and cancer. *Immunity.* 2019;50(2):302–316. doi:10.1016/j.immuni.2019.01.020.
- Villarreal DO, L'Huillier A, Armington S, Mottershead C, Filippova EV, Coder BD, Petit RG, Princiotta MF. Targeting CCR8 induces protective antitumor immunity and enhances vaccine-induced responses in colon cancer. *Cancer Res.* 2018;78(18):5340–5348. doi:10.1158/0008-5472.CAN-18-1119.
- Kamada T, Togashi Y, Tay C, Ha D, Sasaki A, Nakamura Y, Sato E, Fukuoka S, Tada Y, Tanaka A. et al. PD-1 + regulatory T cells amplified by PD-1 blockade promote hyperprogression of cancer. *Proc Natl Acad Sci U S A.* 2019;116(20):9999–10008. doi:10.1073/pnas.1822001116.
- Fourcade J, Sun Z, Chauvin J-M, Ka M, Davar D, Pagliano O, Wang H, Saada S, Menna C, Amin R. et al. CD226 opposes TIGIT to disrupt Tregs in melanoma. *JCI Insight.* 2018;3(14). doi:10.1172/jci.insight.121157.
- Jie HB, Gildener-Leapman N, Li J, Srivastava RM, Gibson SP, Whiteside TL, Ferris RL. Intratumoral regulatory T cells upregulate immunosuppressive molecules in head and neck cancer patients. *Br J Cancer.* 2013;109(10):2629–2635. doi:10.1038/bjc.2013.645.
- Miquelotti LB, Sari MHM, Ferreira LM. Immunotherapy in cancer management: a literature review of clinical efficacy of pembrolizumab in the non-small cell lung cancer treatment. *Adv Pharm Bull.* 2023;13(1):88–95. doi:10.34172/apb.2023.007.
- Stafford M, Kaczmar J. The neoadjuvant paradigm reinvigorated: a review of pre-surgical immunotherapy in HNSCC. *Cancers Head Neck.* 2020;5(1):4. doi:10.1186/s41199-020-00052-8.
- Steven A, Fisher SA, Robinson BW. Immunotherapy for lung cancer. *Respirology.* 2016;21(5):821–33. doi:10.1111/resp.12789.
- Debien V, De Caluwé A, Wang X, Piccart-Gebhart M, Tuohy VK, Romano E, Buisseret L. Immunotherapy in breast cancer: an overview of current strategies and perspectives. *NPJ Breast Cancer.* 2023;9(1):7. doi:10.1038/s41523-023-00508-3.

13. Shi MW, Huang J, Sun Y. Neoadjuvant immunotherapy for head and neck squamous cell carcinoma: expecting its application in temporal bone squamous cell carcinoma. *Curr Med Sci.* 2023;43(2):213–222. doi:10.1007/s11596-023-2700-2.
14. Zhang X, Zhang C, Hou H, Zhang Y, Jiang P, Zhou H, Wang L, Zhou N, Zhang X. Neoadjuvant PD-1 blockade plus chemotherapy versus chemotherapy alone in locally advanced stage II-III gastric cancer: a single-centre retrospective study. *Transl Oncol.* 2023;31:101657. doi:10.1016/j.tranon.2023.101657.
15. Yang Y, Li H, Chen X, Qin J, Li Y, Shen Y, Zhang R, Kang X, Wang Z, Zheng Q. et al. Comparison of neoadjuvant nab-paclitaxel plus immunotherapy versus paclitaxel plus immunotherapy for esophageal squamous cell carcinoma. *Thorac Cancer.* 2023;14(7):700–708. doi:10.1111/1759-7714.14795.
16. Wang K, Liang Y, Huang J, Xie X, Wu D, Chen B, Wang K, Shen Z, Li Y, Wang W. et al. A propensity score-matched analysis of neoadjuvant chemoimmunotherapy versus surgery alone for locally advanced esophageal squamous cell carcinoma. *J Surg Oncol.* 2023;128(2):207–217. doi:10.1002/jso.27277.
17. Ge F, Huo Z, Cai X, Hu Q, Chen W, Lin G, Zhong R, You Z, Wang R, Lu Y. et al. Evaluation of clinical and safety outcomes of neoadjuvant immunotherapy combined with chemotherapy for patients with resectable esophageal cancer: a systematic review and meta-analysis. *JAMA Netw Open.* 2022;5(11):e2239778. doi:10.1001/jamanetworkopen.2022.39778.
18. Yilmaz M, Akovali B. Hyperprogression after nivolumab for melanoma: a case report. *J Oncol Pharm Pract.* 2020;26(1):244–251. doi:10.1177/1078155219845436.
19. Wakiyama H, Kato T, Furusawa A, Okada R, Inagaki F, Furumoto H, Fukushima H, Okuyama S, Choyke PL, Kobayashi H. et al. Treg-dominant tumor microenvironment is responsible for hyperprogressive disease after PD-1 blockade therapy. *Cancer Immunol Res.* 2022;10(11):1386–1397. doi:10.1158/2326-6066.CIR-22-0041.
20. Kashef J, Franz CM. Quantitative methods for analyzing cell-cell adhesion in development. *Dev Biol.* 2015;401(1):165–174. doi:10.1016/j.ydbio.2014.11.002.
21. Zhang X, Peng L, Luo Y, Zhang S, Pu Y, Chen Y, Guo W, Yao J, Shao M, Fan W. et al. Dissecting esophageal squamous-cell carcinoma ecosystem by single-cell transcriptomic analysis. *Nat Commun.* 2021;12(1):5291. doi:10.1038/s41467-021-25539-x.
22. Zheng L, Qin S, Si W, Wang A, Xing B, Gao R, Ren X, Wang L, Wu X, Zhang J. et al. Pan-cancer single-cell landscape of tumor-infiltrating T cells. *Science.* 2021;374(6574):abe6474. doi:10.1126/science.abe6474.
23. Luoma AM, Suo S, Wang Y, Gunasti L, Porter CBM, Nabils N, Tadros J, Ferretti AP, Liao S, Gurer C. et al. Tissue-resident memory and circulating T cells are early responders to pre-surgical cancer immunotherapy. *Cell.* 2022;185(16):2918–2935 e29. doi:10.1016/j.cell.2022.06.018.
24. Hao Y, Hao S, Andersen-Nissen E, Mauck WM, Zheng S, Butler A, Lee MJ, Wilk AJ, Darby C, Zager M. et al. Integrated analysis of multimodal single-cell data. *Cell.* 2021;184(13):3573–3587 e29. doi:10.1016/j.cell.2021.04.048.
25. Stuart T, Butler A, Hoffman P, Hafemeister C, Papalexi E, Mauck WM, Hao Y, Stoeckius M, Smibert P, Satija R. Comprehensive Integration of single-cell data. *Cell.* 2019;177(7):1888–1902 e21. doi:10.1016/j.cell.2019.05.031.
26. Butler A, Hoffman P, Smibert P, Papalexi E, Satija R. Integrating single-cell transcriptomic data across different conditions, technologies, and species. *Nat Biotechnol.* 2018;36(5):411–420. doi:10.1038/nbt.4096.
27. Wu T, Hu E, Xu S, Chen M, Guo P, Dai Z, Feng T, Zhou L, Tang W, Zhan L. et al. clusterProfiler 4.0: a universal enrichment tool for interpreting omics data. *Innov.* 2021;2(3):100141. doi:10.1016/j.xinn.2021.100141.
28. Yu G, Wang L-G, Han Y, He Q-Y. clusterProfiler: an R package for comparing biological themes among gene clusters. *Omics.* 2012;16(5):284–287. doi:10.1089/omi.2011.0118.
29. Trapnell C, Cacchiarelli D, Grimsby J, Pokharel P, Li S, Morse M, Lennon NJ, Livak KJ, Mikkelsen TS, Rinn JL. et al. The dynamics and regulators of cell fate decisions are revealed by pseudotemporal ordering of single cells. *Nat Biotechnol.* 2014;32(4):381–386. doi:10.1038/nbt.2859.
30. Borchertding N, Bormann NL, Kraus G. scRepertoire: an R-based toolkit for single-cell immune receptor analysis. *F1000Res.* 2020;9:47. doi:10.12688/f1000research.22139.1.
31. Liu W, Xie L, He Y-H, Wu Z-Y, Liu L-X, Bai X-F, Deng D-X, Xu X-E, Liao L-D, Lin W. et al. Large-scale and high-resolution mass spectrometry-based proteomics profiling defines molecular subtypes of esophageal cancer for therapeutic targeting. *Nat Commun.* 2021;12(1):4961. doi:10.1038/s41467-021-25202-5.
32. Gerner MC, Ziegler LS, Schmidt RLJ, Krenn M, Zimprich F, Uyanik-Ünal K, Konstantopoulou V, Derdak S, Del Favero G, Schwarzinger I. et al. The TGF- $\beta$ /SOX4 axis and ROS-driven autophagy co-mediate CD39 expression in regulatory T-cells. *FASEB J.* 2020;34(6):8367–8384. doi:10.1096/fj.201902664.
33. Watanabe N, Mo F, Zheng R, Ma R, Bray VC, van Leeuwen DG, Sritabal-Ramirez J, Hu H, Wang S, Mehta B. et al. Feasibility and preclinical efficacy of CD7-unedited CD7 CAR T cells for T cell malignancies. *Mol Ther.* 2023;31(1):24–34. doi:10.1016/j.ymthe.2022.09.003.
34. Zheng Y, Josefowicz SZ, Kas A, Chu T-T, Gavin MA, Rudensky AY. Genome-wide analysis of Foxp3 target genes in developing and mature regulatory T cells. *Nature.* 2007;445(7130):936–940. doi:10.1038/nature05563.
35. Bai M, Grieshaber-Bouyer R, Wang J, Schmider AB, Wilson ZS, Zeng L, Halyabar O, Godin MD, Nguyen HN, Levescot A. et al. CD177 modulates human neutrophil migration through activation-mediated integrin and chemoreceptor regulation. *Blood.* 2017;130(19):2092–2100. doi:10.1182/blood-2017-03-768507.
36. Kim MC, Borchertding N, Ahmed KK, Voigt AP, Vishwakarma A, Kolb R, Kluz PN, Pandey G, De U, Drashansky T. et al. CD177 modulates the function and homeostasis of tumor-infiltrating regulatory T cells. *Nat Commun.* 2021;12(1):5764. doi:10.1038/s41467-021-26091-4.
37. Plitas G, Konopacki C, Wu K, Bos PD, Morrow M, Putintseva E, Chudakov D, Rudensky A. Regulatory T cells exhibit distinct features in human breast cancer. *Immunity.* 2016;45(5):1122–1134. doi:10.1016/j.immuni.2016.10.032.
38. Zheng Y, Chen Z, Han Y, Han L, Zou X, Zhou B, Hu R, Hao J, Bai S, Xiao H. et al. Immune suppressive landscape in the human esophageal squamous cell carcinoma microenvironment. *Nat Commun.* 2020;11(1):6268. doi:10.1038/s41467-020-20019-0.
39. Lowther DE, Goods BA, Lucca LE, Lerner BA, Raddassi K, van Dijk D, Hernandez AL, Duan X, Gunel M, Coric V. et al. PD-1 marks dysfunctional regulatory T cells in malignant gliomas. *JCI Insight.* 2016;1(5):1(5). doi:10.1172/jci.insight.85935.
40. Sawant DV, Yano H, Chikina M, Zhang Q, Liao M, Liu C, Callahan DJ, Sun Z, Sun T, Tabib T. et al. Adaptive plasticity of IL-10(+) and IL-35(+) T(reg) cells cooperatively promotes tumor T cell exhaustion. *Nat Immunol.* 2019;20(6):724–735. doi:10.1038/s41590-019-0346-9.
41. Fridman WH, Meylan M, Petitprez F, Sun C-M, Italiano A, Sautès-Fridman C. B cells and tertiary lymphoid structures as determinants of tumour immune contexture and clinical outcome. *Nat Rev Clin Oncol.* 2022;19(7):441–457. doi:10.1038/s41571-022-00619-z.
42. Chen L, He Q, Zhai Y, Deng M. Single-cell RNA-seq data semi-supervised clustering and annotation via structural regularized domain adaptation. *Bioinformatics.* 2021;37(6):775–784. doi:10.1093/bioinformatics/btaa908.
43. Kumagai S, Koyama S, Itahashi K, Tanegashima T, Lin Y-T, Togashi Y, Kamada T, Irie T, Okumura G, Kono H. et al. Lactic acid promotes PD-1 expression in regulatory T cells in highly glycolytic tumor microenvironments. *Cancer Cell.* 2022;40(2):201–218 e9. doi:10.1016/j.ccell.2022.01.001.

44. Sachs UJ, Andrei-Selmer CL, Maniar A, Weiss T, Paddock C, Orlova VV, Choi EY, Newman PJ, Preissner KT, Chavakis T. et al. The neutrophil-specific antigen CD177 is a counter-receptor for platelet endothelial cell adhesion molecule-1 (CD31). *J Biol Chem.* 2007;282(32):23603–12. doi:10.1074/jbc.M701120200.
45. Saito T, Nishikawa H, Wada H, Nagano Y, Sugiyama D, Atarashi K, Maeda Y, Hamaguchi M, Ohkura N, Sato E. et al. Two FOXP3(+)/CD4(+) T cell subpopulations distinctly control the prognosis of colorectal cancers. *Nat Med.* 2016;22(6):679–684. doi:10.1038/nm.4086.
46. Whiteside SK, Grant FM, Gyori DS, Conti AG, Imianowski CJ, Kuo P, Nasrallah R, Sadiyah F, Lira SA, Tacke F. et al. CCR8 marks highly suppressive Treg cells within tumours but is dispensable for their accumulation and suppressive function. *Immunology.* 2021;163(4):512–520. doi:10.1111/imm.13337.
47. Kidani Y, Nogami W, Yasumizu Y, Kawashima A, Tanaka A, Sonoda Y, Tona Y, Nashiki K, Matsumoto R, Hagiwara M. et al. CCR8-targeted specific depletion of clonally expanded Treg cells in tumor tissues evokes potent tumor immunity with long-lasting memory. *Proc Natl Acad Sci USA.* 2022;119(7). doi:10.1073/pnas.2114282119.
48. Zhu J, Wang Y, Li D, Zhang H, Guo Z, Yang X. Interleukin-35 promotes progression of prostate cancer and inhibits anti-tumour immunity. *Cancer Cell Int.* 2020;20(1):487. doi:10.1186/s12935-020-01583-3.
49. Dieterich LC, Tacconi C, Ducoli L, Detmar M. Lymphatic vessels in cancer. *Physiol Rev.* 2022;102(4):1837–1879. doi:10.1152/physrev.00039.2021.
50. Bayat B, Werth S, Sachs UJH, Newman DK, Newman PJ, Santoso S. Neutrophil transmigration mediated by the neutrophil-specific antigen CD177 is influenced by the endothelial S536N dimorphism of platelet endothelial cell adhesion molecule-1. *J Immunol.* 2010;184(7):3889–3896. doi:10.4049/jimmunol.0903136.
51. Marski M, Kandula S, Turner JR, Abraham C. CD18 is required for optimal development and function of CD4+CD25+ T regulatory cells. *J Immunol.* 2005;175(12):7889–7897. doi:10.4049/jimmunol.175.12.7889.
52. Singh K, Gatzka M, Peters T, Borkner L, Hainzl A, Wang H, Sindrilaru A, Scharffetter-Kochanek K. Reduced CD18 levels drive regulatory T cell conversion into Th17 cells in the CD18<sup>hypo</sup> PL/J mouse model of psoriasis. *J Immunol.* 2013;190(6):2544–2553. doi:10.4049/jimmunol.1202399.